

SOFT X-RAY EMISSION FROM THE RADIO PULSAR PSR 0656+14

F. A. CÓRDOVA,^{1,2} R. M. HJELLMING,³ K. O. MASON,^{4,5} AND J. MIDDLEDITCH¹

Received 1988 December 22; accepted 1989 March 15

ABSTRACT

Using the VLA, we have found a radio source with a flux density of a few mJy in the error region of the soft X-ray source E0656+14. The radio source has a steep, nonthermal spectrum and a high degree of linear (62%) and circular (19%) polarization and is the radio pulsar PSR 0656+14. There is no optical counterpart to the X-ray source to a limit of 23 mag in the *B* band. The X-ray spectrum of the pulsar is among the softest sources observed with the *Einstein Observatory*. There is no indication that the X-ray source is extended. The X-ray data permit a range of blackbody temperatures of $3\text{--}6 \times 10^5$ K, and an equivalent column density of hydrogen $< 4 \times 10^{20}$ cm⁻². If the assumption is made that the X-ray flux is thermal radiation from the surface of the neutron star, then the pulsar must be at a distance < 550 pc. This distance is consistent with the low dispersion measure of PSR 0656+14. There is some suggestion in the X-ray timing data that the X-ray emission is modulated at the pulsar's 0.385 s spin period with an amplitude of $18\% \pm 6\%$. The probability that this is spurious is 0.0002. It was noted by Nousek *et al.* that PSR 0656+14 is close to the geometric center of a 20° diameter soft X-ray-emitting "ring" called the Gemini-Monoceros enhancement. The close distance of the pulsar, together with its relatively young age of 1.1×10^5 yr, make it possible that the ring is a supernova remnant resulting from the explosion of the pulsar's progenitor. A radio source extending over a region 1:2 to 3:3 south of the pulsar is a candidate for association with the pulsar.

Subject headings: nebulae: supernova remnants — polarization — pulsars —
 stars: individual (PSR 0656+14) — stars: neutron — stars: radio radiation —
 X-rays: sources

I. INTRODUCTION

a) The Survey

The X-ray source E0656+14 was discovered in a survey of the ultrasoft sources in the *Einstein Observatory* data base, which covered the energy region 0.15–4 keV (Córdova, Bell, and Kolb 1985; Córdova *et al.* 1989). The intent of the survey was to search for isolated neutron stars with temperatures less than a few $\times 10^5$ K. The survey was done in the following way: X-ray pulse-height data from a large, selected sample of well-known sources (AGN, OB stars, white dwarfs, dwarf novae, etc.) were grouped into three broad energy bands, 0.16–0.56 keV, 0.5–1.08 keV, and 1.08–3.5 keV, and plotted on an X-ray "color-color" diagram. On this diagram the ratio of the counts in the medium-energy channel to the low-energy channel is plotted against the ratio of the counts in the high-energy channel to the low-energy channel. The data were taken with the *Einstein* Imaging Proportional Counter (IPC). Model spectra were folded through the response of this detector and similarly plotted on the diagram. Of our selected "calibration" objects, only a few isolated white dwarfs fell on the "interesting" region of the diagram, i.e., with blackbody spectra having temperatures of the order of a few hundred thousand degrees. Then sources from two *Einstein* surveys, the Medium Sensitivity Survey of Maccacaro *et al.* (1982) and the Galactic Plane Survey of Hertz (1983) were used for a prelimi-

nary soft survey. Of the objects in these surveys, we found only one that was "interesting." The identification of this object, E0656+14, with the radio pulsar PSR 0656+14 was first reported by Córdova *et al.* (1987) and is the subject of this paper.

b) The Discovery

E0656+14 was observed in an *Einstein* survey of the fields of nearby radio pulsars by one of the *Einstein Observatory* Consortium groups. The particular IPC field in which E0656+14 was detected was an observation of the radio error region of PSR 0656+14. E0656+14 was the brightest object detected in the $1^\circ \times 1^\circ$ IPC field of view, yet it was not initially associated with the radio pulsar because the IPC position differed by almost 4' in declination from the best radio position then available (see Table 1). The uncertainty in the radio position was, however, 10' in total extent along the declination direction (Manchester and Taylor 1981), so the X-ray source was still well within the radio error region. The IPC standard processing signaled as a possible identification not the radio pulsar, but a 15th mag variable star, GV Gem, whose position as listed in the General Catalogue of Variable Stars (Kholopov *et al.* 1985, hereafter GCVS) placed it about 1' from the IPC centroid position. When we measured the position of GV Gem accurately, however (based on the finding chart referenced in the GCVS), we found that it is actually about 3' from the IPC position (Table 1). We noted Hertz's (1983) comments that there was an HRI image of the source and since there was no optical counterpart at the HRI position on the POSS Survey prints, we initiated our own optical search for a counterpart using deep CCD images. As we still found no optical candidate to a deeper limit (see below), we decided to pursue radio observations, suspecting that the E0656+14 might indeed be the radio pulsar PSR 0656+14. This venture proved fruitful since we found a radio source 4" from the centroid of the HRI posi-

¹ Los Alamos National Laboratory.

² Guest User of the NRAO Very Large Array, which is operated by Associated Universities, Inc., under contract with the National Science Foundation.

³ National Radio Astronomy Observatory, Socorro.

⁴ Mullard Space Science Laboratory, University College London.

⁵ Guest User of the Isaac Newton Telescope, which is operated on the island of La Palma by the Royal Greenwich Observatory in the Spanish Observatorio del Roque del los Muchachos of the Instituto de Astrofísica de Canarias.

TABLE 1
SUMMARY OF POSITIONAL INFORMATION

Source	Instrument	R.A.(1950)	Decl. (1950)
GV Gem	Optical GCVS	06 ^h 56 ^m 59 ^s	14°20'
	Optical measured	06 57 07.2	14°20'48"
PSR 0656 + 14	Molonglo Radio Observatory	06 56 57(2)	14 15 (5)
E0656 + 14	<i>Einstein</i> IPC	06 56 58(2)	14 18 51(35)
	<i>Einstein</i> HRI	06 56 58.0(2)	14 18 31(4)
PSR 0656 + 14	VLA	06 56 57.93(01)	14 18 33.6(2)

tion, whose properties suggested its identity as PSR 0656 + 14. J. Taylor later privately communicated that he and colleagues recently had determined a better radio position for the pulsar, based on pulse-timing data (Dewey *et al.* 1988), and this position coincided with our VLA position. Thus E0656 + 14 is securely identified with PSR 0656 + 14. In § V we demonstrate that it is the softest X-ray-emitting radio pulsar yet discovered.

II. THE OBSERVATIONS

a) X-Ray

The field of E0656 + 14 was observed twice with the *Einstein Observatory*, once with each of the imaging focal plane detectors. The IPC detector, a gas-filled proportional counter, has a spatial resolution of about 1'. The spectral resolution of the detector, $E/\Delta E$, is > 1 between 1.5 and 4 keV, and 0.5 at 0.25 keV. The data are collected in 32 pulse-height channels. The HRI, in contrast, is a digital X-ray camera that has a spatial resolution of about 4" and no energy resolution. The energy passband of both detectors, 0.15–4.5 keV, is determined by the window and mirror cutoffs, but the HRI has a relatively greater response at lower energies: The effective area of the IPC is over 100 cm² between 0.2 keV and 3 keV, but only about 15 cm² at 0.15 keV, while the effective area of the HRI is between 10 and 20 cm² between 0.15 keV and 0.8 keV and is only 1 cm² at 3.5 keV. Details of both detectors are given in Giacconi *et al.* (1979).

The IPC observation, sequence I2486, was made on 1979 April 8 between UT 2:37:40.7 and UT 3:27:30.8. The net time on the source, corrected for gaps and dead time of the instrument, was 1755 s. The net count rate of the source, corrected for background, telescope vignetting, mirror scattering, detector dead time, and the cell size used, was 0.365 ± 0.02 s⁻¹ in the energy band 0.2–3.5 keV. This rate takes into account the fact that the low-energy photons form a larger image of the source than the higher energy counts. The detector and sky background contributed about 2% of the counts in a "detection cell" of 3' radius around the source.

The HRI image of PSR 0656 + 14, sequence H9266, was taken on 1981 March 29 between UT 15:34:59.0 and UT 20:15:33.5. The exposure time on the source was 4728.6 s. The

net count rate was 0.270 ± 0.009 s⁻¹. The background was 1% of the counts in a circle of 18" radius around the source.

b) Optical

Optical images of the E0656 + 14 field were made with a CCD camera at the prime focus of the 2.5 m Isaac Newton Telescope at the Observatorio del Roque de los Muchachos, La Palma, Canary Islands. CCD frames in the *V*, *R*, and *I* bands were taken in 1986 November using a GEC chip. *B*-band observations were made in 1987 February using a more blue sensitive RCA chip. Details of the observations are contained in Table 2. On each night several standard stars were observed using the same instrumental setup as for the X-ray object in order to calibrate the images in terms of an external photometric system.

Figure 1 (Plate 6) shows the *V*-band image of the E0656 + 14 field. Astrometry of several stars in the field allows us to locate the position of the X-ray source on the CCD frame to high accuracy; a box is drawn centered on the source's position in the inset to Figure 1. The sides of this box are 10" long. No optical image was recorded at the position of the pulsar in the *V*-band image, or in the images taken with the other filters. In Table 2 we list the limiting magnitude of the images in each filter. These are the measured magnitudes of the faintest stellar image definitely recorded in each frame. A 15 minute CCD exposure of the field in the *R* band was taken by Jeremy Mould using the 100 inch (2.7 m) telescope at Las Campanas, Chile. He derives a limiting magnitude of $R > 23.3$ for the pulsar.

c) Radio

On 1987 November 3, between 10:22 and 12:52 UT, we made VLA radio observations of the field centered on E0656 + 14. These observations were made with the VLA in its hybrid A/B (20 km) configuration with 50 MHz bandwidth and on-source integration times of 34, 51, and 12 minutes at frequencies of 1.49, 1.64, and 4.9 GHz, respectively. An unresolved radio source was detected at all frequencies at the position $\alpha_{1950} = 6^{\text{h}}56^{\text{m}}57^{\text{s}}.93$, $\delta_{1950} = +14^{\circ}18'33''.6$ with an uncertainty of 0".2. This position was derived assuming that the

TABLE 2
OPTICAL OBSERVATIONS OF PSR 0656 + 14 FIELD

Color	CCD Chip	Date	Exposure Time (s)	Seeing	B/g Counts (per pixel)	Limiting Magnitude
<i>B</i>	RCA	1987 Feb 24	600	1".4	4000	23.1
<i>V</i>	GEC	1986 Nov 26	300	1.0	4800	22.1
<i>R</i>	GEC	1986 Nov 26	200	1.8	7900	21.5
<i>I</i>	GEC	1986 Nov 26	400	2.1	27,000	20.9

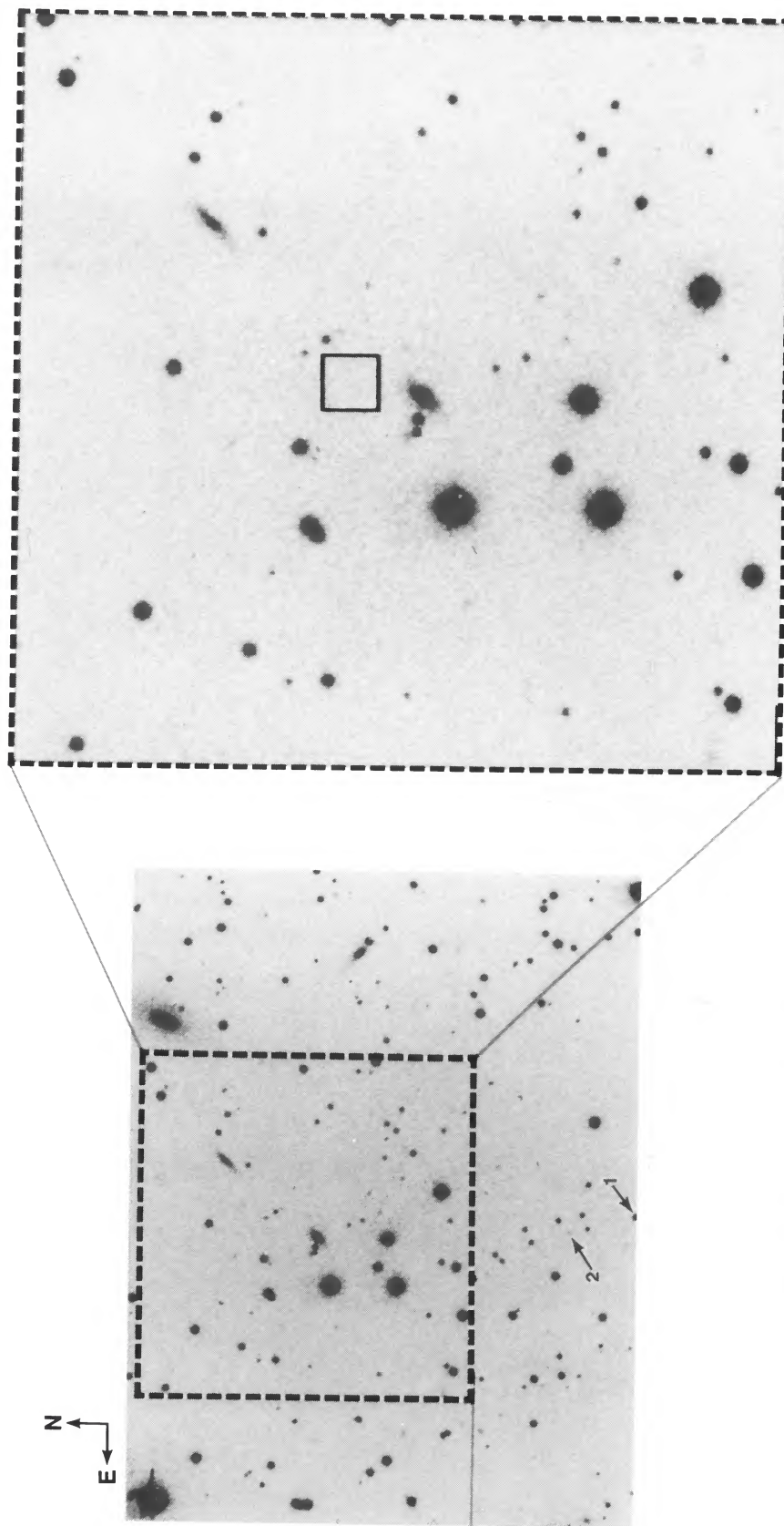


FIG. 1.—CCD V band image of the E0656+14 field. The box drawn in the inset is $10''$ long and centered on the position of the X-ray source. No optical source is detected to a limiting V magnitude of 22.1. Two optical objects, denoted “1” and “2,” are discussed in the text because of their possible relationship to an extended radio source near the pulsar.

CÓRDOVA *et al.* (see 345, 452)

TABLE 3
RADIO PARAMETERS OF PSR 0656 + 14 ON 1987 NOVEMBER 3

Frequency (GHz)	I (mJy)	P (mJy)	V (mJy)	P/I	V/I
1.49	5.8 ± 0.2	3.6 ± 0.2	1.1 ± 0.2	62%	19%
1.64	4.2 ± 0.3	2.4 ± 0.3	0.8 ± 0.3	57	19
4.9	0.65 ± 0.15	<0.2	<0.2

source used for phase calibration, 0735 + 178, had a position of $\alpha_{1950} = 7^{\text{h}}35^{\text{m}}14^{\text{s}}.126$, $\delta_{1950} = +17^{\circ}49'9''.3$, with an uncertainty of 0".1. The position of the unresolved radio source is within the 4" radius HRI error region of E0656 + 14. In Table 3 we summarize various combinations of the I and V Stokes parameters of the source, in addition to the linearly polarized intensity P , for each frequency (ν).

The 1.49 and 4.9 GHz data in Table 3 are based upon the combined 50 MHz-wide bands at 1.465 and 1.515 GHz, and at 4.835 and 4.885 GHz; the 1.665 GHz band was so seriously affected by interference that in this frequency interval only the 50 MHz band centered on 1.635 GHz was usable. The numbers in Table 3 are slightly different from those in the preliminary announcement by Córdoba *et al.* (1987), mainly due to improvements in the data due to self-calibration and removal of data affected by interference. Additional observations, done in right circularly polarized spectral line mode with the C configuration VLA on 1988 April 5–6, showed the presence of the pulsar at a level of 12 ± 0.5 mJy at 1.42 GHz. This is significantly larger than seen on 1987 November 3. This may be because of variability in the average pulsar emission, or there may be a larger fraction of the emission in right circular polarization. Another explanation is that the lower-resolution observations detected broader emission surrounding the pulsar. The latter possibility has been suggested by Nelson and Spencer (1988) who report a flux of 4.6 ± 0.7 mJy for the pulsar when observed with a short-spacing interferometer at 5 GHz, and 0.67 ± 0.11 mJy (essentially the same value listed in Table 3) when observed independently with the VLA at 5 GHz. They also failed to detect pulsed emission at another time, with an upper limit of 2 mJy. Nonpulsed emission from the vicinity of the pulsar may be related to a source which is 2:1 in extent and south of the pulsar, discussed in more detail below.

We see from Table 3 that the radio source has very high linear polarization (62%), high circular polarization (19%), and a steep spectrum of the form $S_{\nu} \propto \nu^{-1.8}$, all of which are characteristic of pulsars (Manchester and Taylor 1981). Based upon the pulsar-like characteristics of the radio source and the positional coincidence with the small X-ray source error region, we identify this object with the pulsar PSR 0656 + 14 originally discovered by Manchester *et al.* (1978) using the Molonglo Radio Telescope.

III. FURTHER X-RAY ANALYSIS

a) The X-Ray Spectrum

As mentioned in the Introduction, the first fact that we knew about the unidentified *Einstein* source E0656 + 14 was that its X-ray spectrum was very soft. This information was based on its location in our X-ray color-color diagram, which was in a region mostly populated by isolated white dwarfs and some accreting, highly magnetic white dwarfs (polars), whose relatively bright *Einstein* spectra have been successfully fit with low-temperature ($kT < 50$ eV), relatively unabsorbed black-

bodies, or steep power laws with spectral indices $\alpha > 2$ (see power-law form below). The X-ray colors of PSR 0656 + 14 are similar to those of the polars 1114 + 18, 0139 – 68, and VV Pup in their high states, α Centauri, Procyon, and the white dwarf EG 187 (Córdoba *et al.* 1989). The pulsar's X-ray colors imply a spectrum somewhat less steep than that of Sirius.

More quantitative constraints on the spectral temperature and column density to PSR 0656 + 14 can be obtained by convolving various spectral models with the response function of the detector and comparing the predicted count distribution (which is normalized to the observed counts over the bandpass of interest) to the IPC pulse-height data. A χ^2 test yields similarly acceptable fits for both blackbody and power-law models, modified by interstellar absorption. Both model fits give a minimum total χ^2 of 6.2 for 6 degrees of freedom. In Figure 2 the shaded areas show the 90% confidence regions for the fits as a function of spectral index and equivalent hydrogen column density N_{H} , using the prescription of Lampton, Margon, and Bowyer (1976) for these two interesting parameters. The blackbody fits are compatible with the data provided that $kT < 0.07$ keV; for $kT > 0.02$ keV; $N_{\text{H}} < 6.0 \times 10^{20}$ cm^{-2} . The power-law fits indicate a value for the spectral index $\alpha > 2.6$ (for a power law of the form $S_{\nu} \propto \nu^{-\alpha}$) and $N_{\text{H}} < 2.0 \times 10^{20}$ cm^{-2} .

The HRI detected the pulsar at a count rate which was 75% that in the IPC detector. Using the published quantum efficiency curves, we have investigated combinations of spectral parameters which would yield the observed count rate ratio between the HRI and IPC. Of the complete range of permissible spectral values computed from the IPC data alone, only certain combinations of kT and N_{H} yield the correct count rate ratio for the energy interval from 0.15 keV to 1.5 keV. The dashed line in Figure 2a shows these combinations. The absolute efficiency of the IPC and HRI detectors is not accurately determined. Accepting an error in the relative absolute efficiencies of 15%, the combinations of kT and N_{H} in the hatched region surrounding the dashed line of Figure 2a are permitted. To allow *any* combination of IPC parameters within the entire 90% confidence area in Figure 2a would require that this uncertainty be as large as 30%. (Note that the errors in the count rates are only a few percent.)

If we postulate that all of the soft X-ray emission comes from the surface of the neutron star, we can further limit the range of permissible blackbody spectral parameters if we know the pulsar's distance. We can require that the observed spectrum of PSR 0656 + 14 does not imply a total luminosity larger than the luminosity of a neutron star whose entire surface is emitting thermal radiation. We consider the luminosity of a neutron star with a radius of 16 km, this radius being representative of a stiff equation of state for a neutron star with a mass between 0.4 and 1.4 M_{\odot} (Pandharipande and Smith 1975). We do not make a relativistic correction to the predicted luminosity because the correction is small (4%–17%) for neutron stars with a stiff equation of state (Gudmundsson, Pethick, and Epstein 1983). We compare the luminosity of such a star with the luminosity implied by the measured data on the pulsar, for different values of kT and N_{H} . Combinations of these parameters that require an emitting area greater than that of a neutron star with a radius of 16 km can be rejected. If the pulsar is at a distance of 400 pc (i.e., estimated from the pulsar's radio dispersion measure of 14 cm^{-3} pc^{-1} , and a model of the mean free electron density in the Galaxy; Manchester and Taylor 1981), then the requirement is met only for a portion of

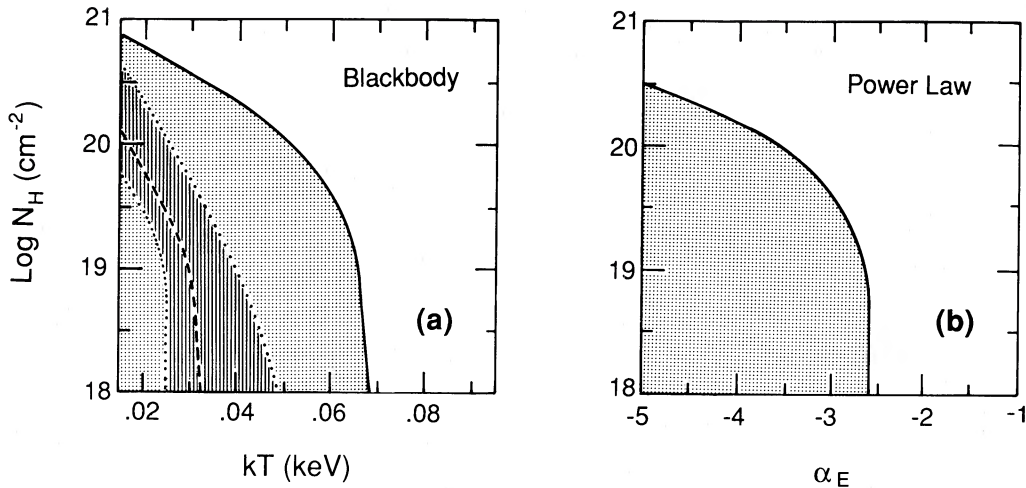


FIG. 2.—The shaded areas show combinations of spectral parameters allowed by fits of blackbody and power-law models to the IPC data on PSR 0656+14. For only certain combinations of kT and N_H do the HRI and IPC give equal observed fluxes; this is represented by the dashed line in (a). The hatched area around this line is for values where the ratio of observed fluxes in the two detectors is within 15%. In (b), α_E represents the spectral index for a power law of the form $S_\nu \propto \nu^{-\alpha_E}$.

the shaded area in Figure 2a bounded by $0.045 \text{ keV} < kT < 0.07 \text{ keV}$ if $N_H = 1.0 \times 10^{18} \text{ cm}^{-2}$, and $0.053 \text{ keV} < kT < 0.07 \text{ keV}$ if $N_H = 1.0 \times 10^{20} \text{ cm}^{-2}$. Including the requirement that the HRI to IPC count rates are compatible (within 15%) further restricts N_H to $\leq 10^{18} \text{ cm}^{-2}$, and the temperature to $kT = 0.045\text{--}0.048 \text{ keV}$ (for $d = 400 \text{ pc}$).

Figure 3 shows the distances allowed by the observed flux data, under the assumption that all the soft emission comes from the neutron star's surface. Using the restriction on kT depicted by the hatched area in Figure 2a (namely, that the fluxes in the HRI and IPC are equal over the same bandpass) puts an upper limit on the distance of 550 pc. This improves the constraint of the IPC pulse-height data alone, which allows kT as great as 0.068 keV, and a distance of about 1 kpc (see Figs. 2a and 3). If the distance to the pulsar is greater than about 550 pc, then the observed flux is too large to be due solely to thermal blackbody emission from the pulsar, and the emitting area must be larger than that of the surface area of a 16 km neutron star.

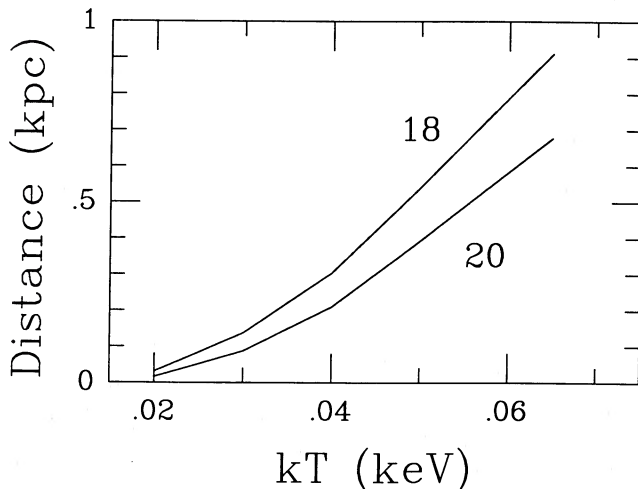


FIG. 3.—The distance of the pulsar as a function of emission temperature is derived for two values of $\log N_H$, assuming that all of the observed X-ray flux comes from blackbody emission from the entire surface of a 16 km radius neutron star.

The flux above 0.15 keV (after correction for interstellar absorption) for a spectrum with $kT = 50 \text{ eV}$ and $N_H = 1.0 \times 10^{18} \text{ cm}^{-2}$ is $3.9 \times 10^{-12} \text{ ergs cm}^{-2} \text{ s}^{-1}$. For a distance of 400 pc, this corresponds to a luminosity of $7.1 \times 10^{31} \text{ ergs s}^{-1}$. The total luminosity, i.e., integrated over all frequencies, would be $1.2 \times 10^{32} \text{ ergs s}^{-1}$. The range of observed flux values consistent with the entire permitted kT - N_H region in Figure 2a is $(2\text{--}10) \times 10^{-12} \text{ ergs cm}^{-2} \text{ s}^{-1}$, or a luminosity of $(0.36\text{--}1.8) \times 10^{32} \times (d/400 \text{ pc})^2 \text{ ergs s}^{-1}$ for $E > 0.15 \text{ keV}$.

The best-fit power law model is for $\alpha = 4$, $N_H = 5 \times 10^{18} \text{ cm}^{-2}$. The flux between 0.15 and 3.5 keV, corrected for absorption losses implied by the best fit N_H , is $2.6 \times 10^{-12} \text{ ergs cm}^{-2} \text{ s}^{-1}$, or a luminosity of $5 \times 10^{31} \times (d/400 \text{ pc})^2 \text{ ergs s}^{-1}$.

b) Search for Extended X-Ray Emission

We have shown above that data on the soft X-ray spectral shape and luminosity of PSR 0656+14 are consistent with the hypothesis that the observed emission is thermal radiation from the surface of a neutron star. However, many of the X-ray-emitting pulsars detected are measurably extended sources in the *Einstein* HRI detector, indicating that the X-rays are, for the most part, due to a plerionic component (see Seward and Wang 1988). To search for possible extended emission associated with the PSR 0656+14 we analyzed the HRI spatial data, using the *Einstein* Data Center software. We plot in Figure 4 the surface brightness profiles of the pulsar and an oft-used X-ray "standard" for the point source response, 3C 273, as a function of radius. The data have been normalized so that they closely fit the carbon calibration curve for values less than $5''$. The data on 3C 273 provide an excellent fit to the point response of the carbon calibration source. The first point for the pulsar (i.e., the surface brightness for an annulus between $0''$ and $2''$) is discrepant, perhaps due to jitter in the aspect, but the remaining data also fit closely the point response curve. There is no evidence that the pulsar's X-ray emission is extended for radii between about $5''$ and about $40''$ (Fig. 4 shows that the pulsar's X-ray intensity and the detector background are approximately equal at $45''$).

c) X-Ray Timing Analysis

Both the IPC and HRI data for E0656+14 have gaps where no counts could be recorded due to Earth occultations and

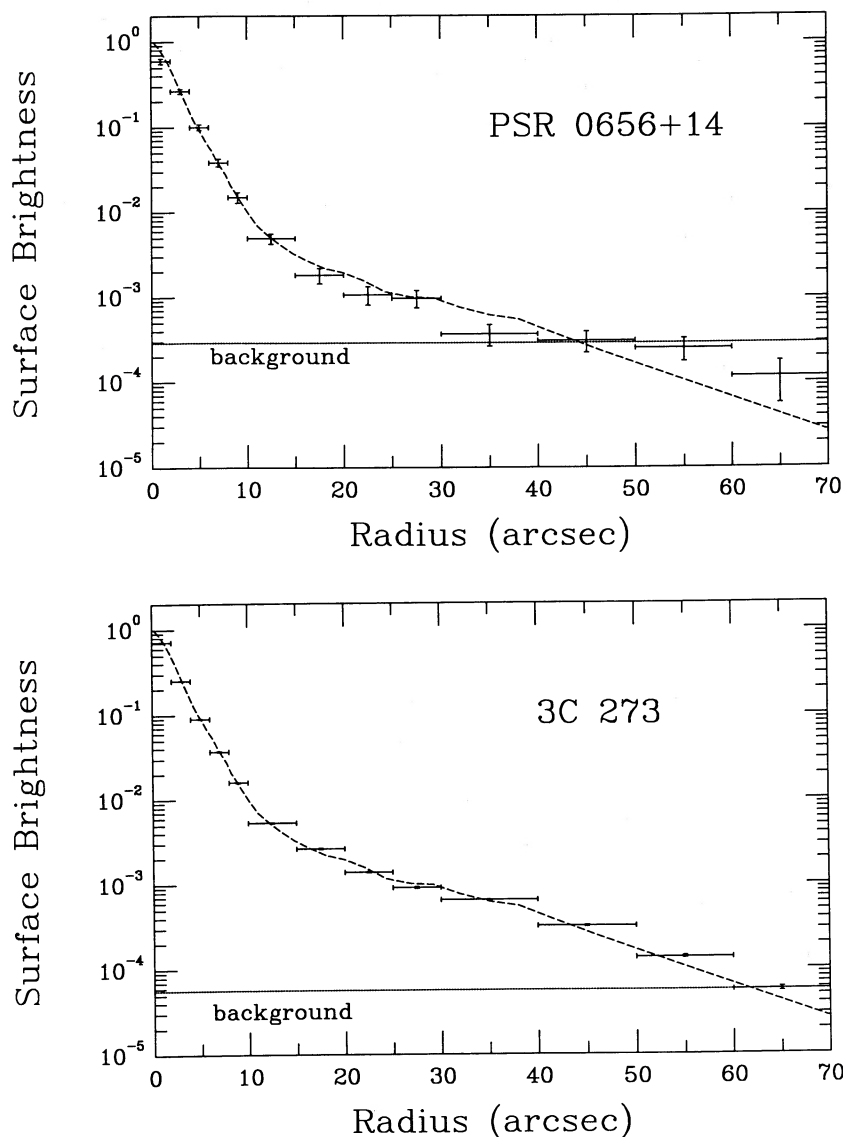


FIG. 4.—Surface brightness profiles. The X-ray data from the pulsar and 3C 273 (for comparison) are normalized for values less than $5''$ to the carbon calibration point source response curve to search for evidence of extended emission.

passages through the South Atlantic Anomaly, etc. Any further (short) dropouts have been padded with the local mean value, and the resulting time series are plotted in Figure 5. The data were tested against the hypothesis that the count rate is constant and yielded χ^2 values of ~ 16 for 13 IPC points and ~ 17 for 15 HRI points—consistent with less than 20% variability over time scales of 40 minutes for the IPC and over a few hours for the HRI.

In order to test the E0656+14 data for pulsations with the same frequency as the radio pulsar, PSR 0656+14, the IPC and HRI data were each incorporated into separate time series which were then Fourier-analyzed. For the IPC data, only events in pulse-height channels corresponding to energies where the pulsar's contribution substantially exceeds the contribution from the background, that is, between 0.16 and 0.8 keV, were included in the analysis (i.e., 674 events). The interpolated power spectra from the Fourier transforms were then examined for excess power at the radio pulsar frequencies corresponding to the IPC and HRI observation epochs (2.598321

Hz and 2.598298 Hz, respectively—see Fig. 6). Power amounting to 7.1 and 3.8 times the local mean level was seen at these frequencies in the two spectra (Fig. 6), an occurrence which would happen in the absence of a signal with a probability of ~ 0.0002 . No significant harmonic structure was observed in either power spectrum: the fourth harmonic in the IPC spectrum and the second harmonic in the HRI spectrum have about twice the mean power level, and all other harmonics through the fifth harmonic have less power. The equivalent pulsed fractions derived from the power at the fundamental frequencies of the two data sets are 17.8% (IPC) and 11.2% (HRI), with an error of 6% in each case. (The background count rate is negligible in both detectors.)

We also examined the pulse profiles for the two data sets, which are shown in Figure 7, with the same data (13 bins) repeated twice in each profile for purposes of clarity. These pulse profiles have been plotted so that the peak of the 2.6 Hz fundamental frequency, as derived from a fit to each pulse profile, occurs at phase 0.0. The fourth harmonic structure in

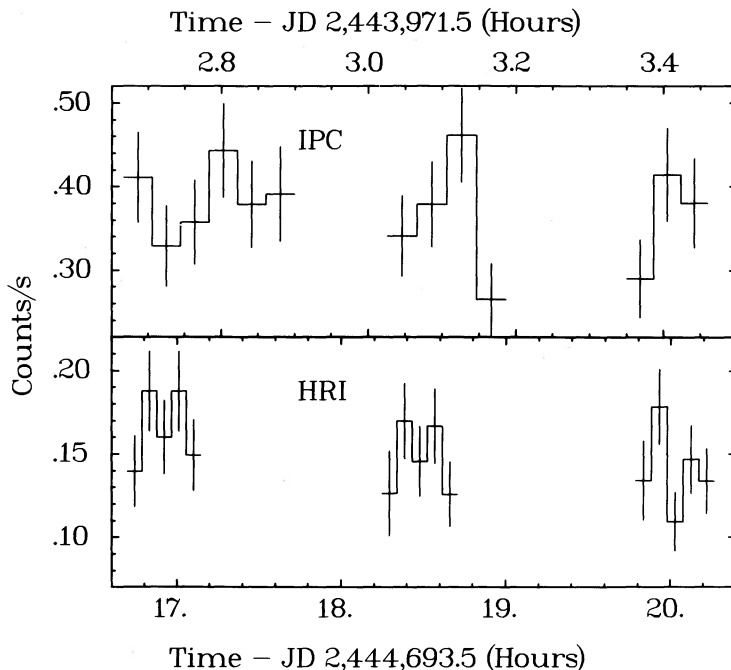


FIG. 5.—The time history of the HRI count rate in bins of ~ 350 s (*lower*) and the IPC count rate in bins of ~ 140 s (*upper*). The rates have been corrected for the small dropouts occurring within the plotted time intervals. The 1σ errors for each interval are also shown.

the IPC data is clearly seen to arise from the two high bins near phases 0.7 and 0.9 cycles, while the second harmonic structure is evident in the HRI pulse profile. However, the Fourier transform statistics imply that neither of these structures is significant, and indeed most of it disappears when the two pulse profiles are summed in the top frame of Figure 7. The sinusoidal shape of the X-ray pulse profile is similar to that of PSR

1509–58 in MSH 15–52 and the LMC pulsar (Seward and Harnden 1982; Seward, Harnden, and Helfand 1984).

IV. THE EXTENDED RADIO EMISSION

Figure 8 contains three images of the pulsar and other radio sources in the central $4'$ portion of the 0.5° antenna beam. The pulsar is the only circularly polarized radio source in the entire

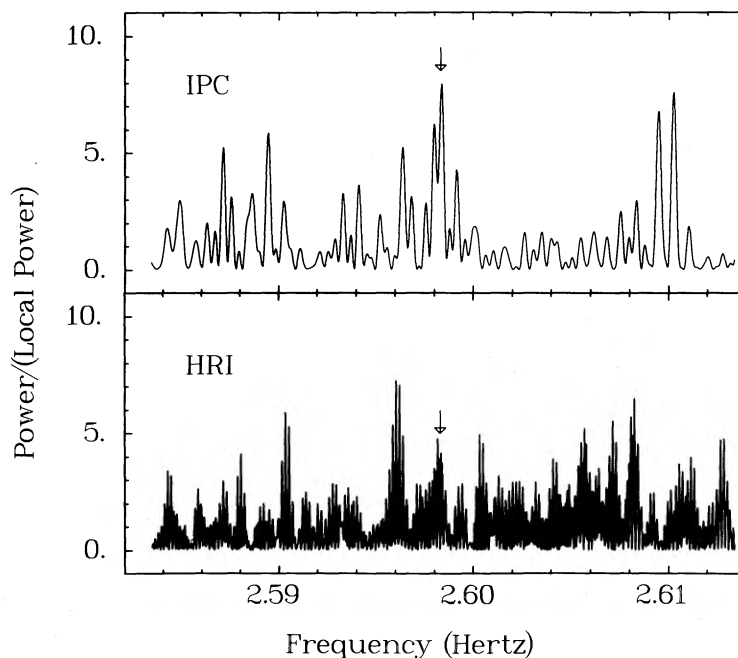


FIG. 6.—Sections of the interpolated power spectra near the PSR 0656+14 pulse frequency (*arrows*) derived from the HRI data (*lower*) and from the IPC data (*upper*). The power level of the IPC spectrum at the PSR 0656+14 frequency is 7.1, while the corresponding power level of the HRI spectrum is 3.8 (the expected mean power due to noise alone is 1.0).

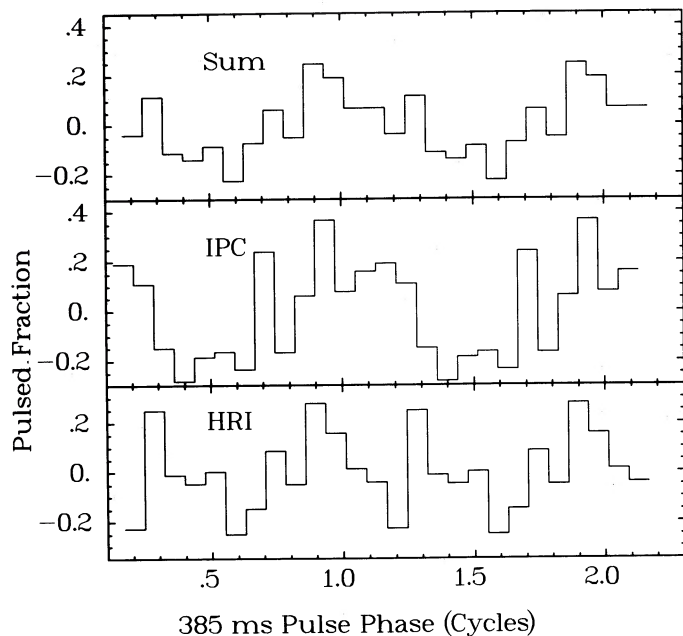


FIG. 7.—The pulse profiles derived from the HRI (*lower*) and IPC (*middle*) data at the expected pulse frequency of PSR 0656+14 (see Fig. 6). The profiles are shown repeated for one extra cycle for purposes of clarity. The pulse profiles have been aligned so that the maximum of the 385 ms Fourier component occurs at phase 1.0. The sum of the two profiles is shown in the upper frame.

antenna beam (see Fig. 8a for the Stokes V parameter image of the central portion of the beam; the “noise” level in this image is consistent with the expected residuals due to the defects, introduced by the off-axis feeds, in the circularly polarized beams of the VLA antennas). The synthesized beam for Figure 8a is $5''.2 \times 3''.0$ with major axis at position angle -85° ; the pulsar image reflects this beam shape. Figure 8b is the Stokes I parameter image of the same field. It shows the pulsar, an unusual large and extended radio source $85''$ south of the pulsar, and another source $85''$ farther south. This image was obtained with natural weighting and a taper of 30,000 wavelengths, in order to emphasize broader structures, giving a synthesized beam of $7''.2 \times 6''.1$ with a major axis at position angle -29° . Figure 8c is an image of linearly polarized intensity derived from $P = (U^2 + Q^2)^{1/2}$, where U and Q are the linear polarization Stokes parameter images. It shows the high (62%) linear polarization of the pulsar, the 12% linear polarization of the peak of the most southerly source in the image, and the extended linear polarization image of the central source. Parts of the latter are 40%–50% linearly polarized.

A number of pulsars are known to be associated with diffuse synchrotron-emitting nebulae. Therefore it is important to determine if the extended radio source near PSR 0656+14 is related to the pulsar.

Because of the low distance estimate to PSR 0656+14, based on its low dispersion measure and the ultrasoft X-ray emission of E0656+14, anything associated with the pulsar should be no more than a few hundred parsecs distant. In particular, the neutral hydrogen column density should be small. We used the VLA in its C and D arrays to search for 21 cm hydrogen (H I) absorption features against both the complex of strong, extended radio emission $70''$ – $200''$ south of the pulsar and next brightest source complex in the antenna beam, which is located $6'$ south and $6'$ west of the pulsar.

Presence of significant absorption features would indicate the radio emission is distant and presumably outside our Galaxy, whereas lack of absorption features would indicate the radio sources were nearby and possibly associated with the pulsar.

The H I line observations were made from 20:00 UT on 1988 April 5 to 08:00 UT on April 6 with the C (3.5 km) configuration of the VLA and on 1988 July 12 from 14:30 to 20:30 UT with the D (1 km) configuration. All observations were made using a spectral line mode with 32 channels at separations of 24.4 kHz corresponding to 5 km s^{-1} intervals. This covers the H I velocity range of -60 to $+90 \text{ km s}^{-1}$, Doppler-shifted with respect to the H I rest frequency of 1420.406 MHz. An image of the pulsar and nearby radio sources, made by adding all the spectral line channels from the C configuration data, is shown in Figure 9. At this resolution all of the nonpulsar radio emission shown in Figure 8b is seen to be part of one radio source with a north-south extent of $2''.1$.

Figure 10a shows the D array absorption spectrum for the calibrator 0622+147, illustrating the typical deep absorption features produced by cool hydrogen in the interstellar medium. Figure 10b shows the H I absorption spectrum produced by the line of sight to the complex of elongated emission, which is 46 mJy in total strength. No significant absorption is seen with a 3σ upper limit corresponding to an optical depth of 0.08 in each channel. Figure 10c shows the absorption spectrum against the second brightest source in the field, a 36 mJy source which is the combination of the three sources in the lower right corner of Figure 9. A weak absorption feature corresponding to an optical depth of 0.15 is seen in one channel at a velocity of $+35 \text{ km s}^{-1}$. These results correspond to an upper limit of $N_{\text{H}} < 10^{20} (T_s/100 \text{ K}) \text{ cm}^{-2}$ for the hydrogen column density in the line of sight to the $2''.1$ elongated source of Figure 9. The weak absorption against the second brightest source (see Fig. 10c) corresponds to $N_{\text{H}} \sim 1.4 \times 10^{20} (T_s/100) \text{ cm}^{-2}$. For a line of sight through the interstellar medium to the edge of the Galaxy in this direction, $N_{\text{H}} = 1.5 \times 10^{21} \text{ cm}^{-2}$ (A. Stark 1988, private communication; Weaver and Williams 1973). This would suggest that the extended source is indeed nearby and not extragalactic. Unfortunately, the very small N_{H}/T_s in the line of sight to the 36 mJy radio source indicates that we cannot unambiguously come to that conclusion: the interstellar medium along lines of sight near the pulsar may have a very high harmonic spin temperature, i.e., $T_s > 1100 \text{ K}$. Thus the negative result on absorption against the $2''.1$ elongated source south of the pulsar indicates either that this source is nearby or that the H I along this line of sight is unusually devoid of cool H I clouds (see Kulkarni and Heiles 1988).

V. DISCUSSION

a) PSR 0656+14 in the Context of Other X-Ray-emitting Neutron Stars

It is interesting to compare the properties of PSR 0656+14 with those of other X-ray-emitting, isolated neutron stars. A list of a dozen objects which fall into this category is given in Table 4. The table gives for the pulsars the pulsar period, the period derivative, the rotational energy loss rate, $I\Omega\dot{\Omega}$ ($=\dot{E}$), the spin-down age, $P/(2\dot{P})$, and the dispersion measure. It also gives the distances for all the objects, and the ages of the SNR associated with the nonpulsing objects. Seven (possibly eight with PSR 0656+14; see below) of the objects are associated with supernova remnants, and many of the pulsing objects are associated with plerions, which are extended, flat-spectrum

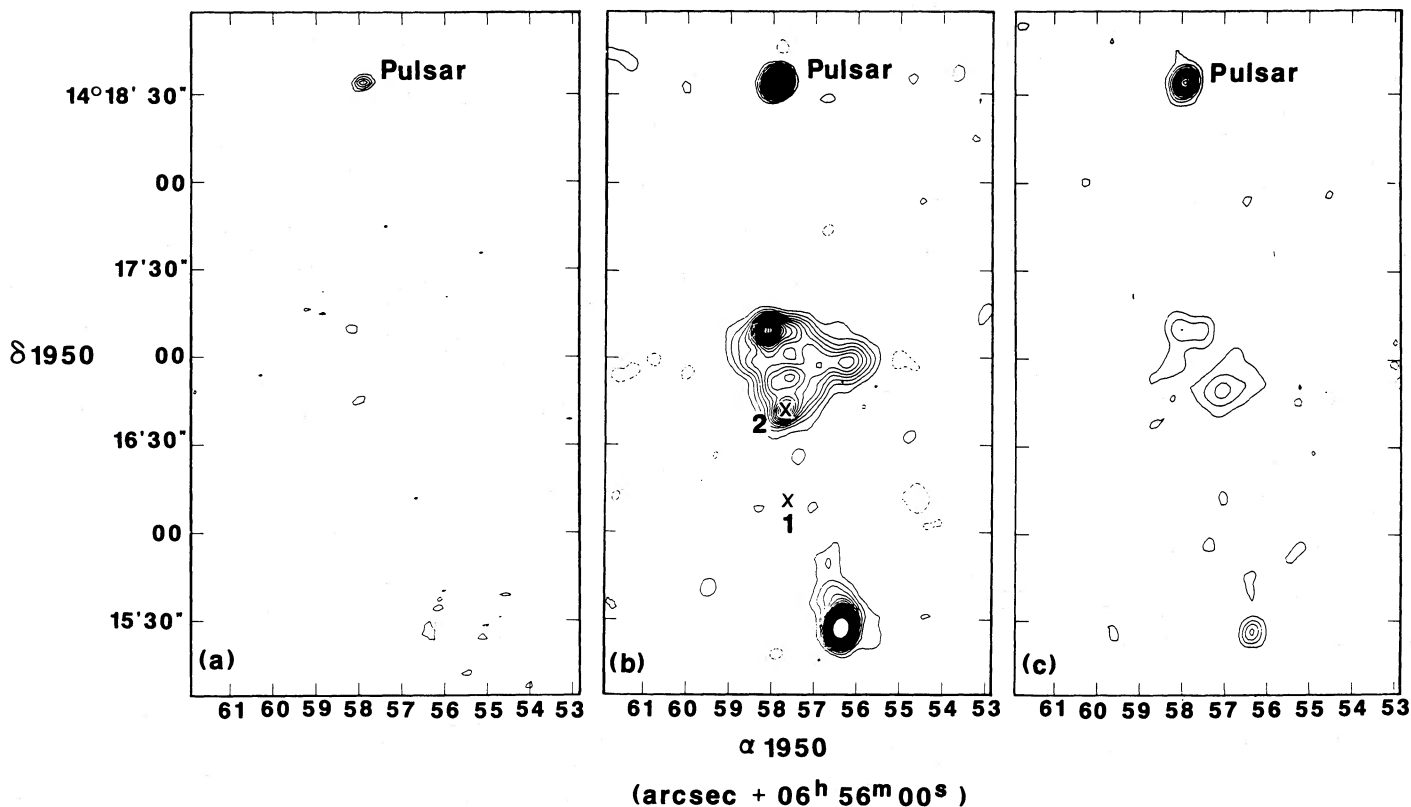


FIG. 8.—Three images of a 4' field that include the pulsar PSR 0656 + 14, made with the VLA A/B configuration at 1.49 GHz: (a) a Stokes V parameter image in which the pulsar is the only circularly polarized (19%) source among the ~ 15 sources in the antenna beam; (b) a Stokes I parameter image with tapering to emphasize broader structures; and (c) a linearly polarized intensity image in which the pulsar is the dominant source in the field because of its 62% linear polarization. Locations denoted "1" and "2" in (b) correspond to the similarly marked positions of optical objects in Fig. 1.

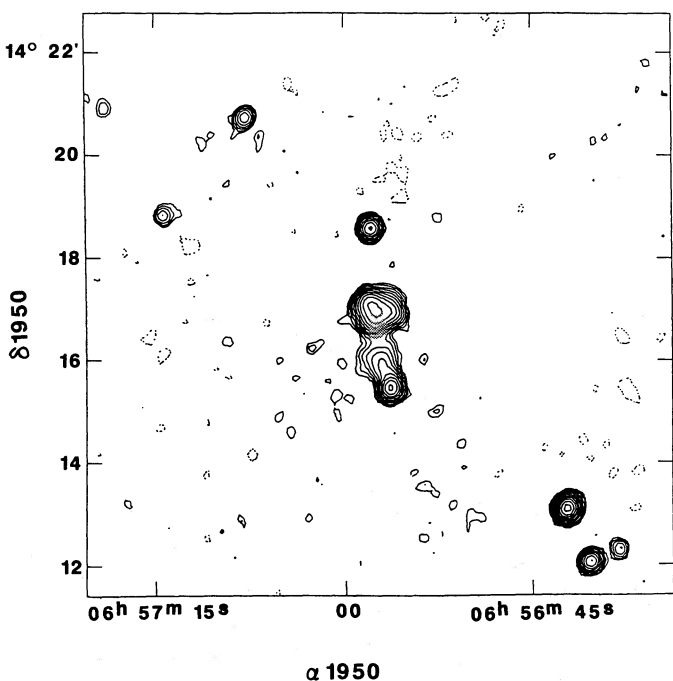


FIG. 9.—An image of an 11' region in the vicinity of PSR 0656 + 14 made with the VLA C configuration at 1.49 GHz on 1988 April 5–6.

radio sources enveloping the pulsars and probably energized by them.

Included in Table 4 is the probable counterpart of the gamma-ray source Geminga. Not included are PSR 1642–03, PSR 0355 + 54, 3C 58, and 2259 + 58 (G109.1–1.0). While claims have been made for X-ray detections of the first two of these, more recent examination of the *Einstein* data suggests that this emission is not coincident with the positions of the pulsars and may be associated instead with synchrotron nebulae (Seward and Wang 1988). High-resolution *Einstein* observations do show a compact source clearly in 3C 58, but it is dominated by the remnant emission (Becker, Helfand, and Szymkowiak 1982) and thus it is not yet possible to provide X-ray spectral parameters for any pulsar which might be present. No radio pulsar has yet been detected in 3C 58. It is difficult to explain the X-ray luminosity of 2259 + 58, a 7 s X-ray pulsar in a semicircular filled X-ray shell, as being powered by the pulsar (\dot{E} is only 10^{32} ergs s^{-1} and the pulsar's X-ray luminosity is $\sim 2 \times 10^{35}$ ergs s^{-1}) unless the pulsar is in a binary system. It is unlikely, therefore, that it is an isolated neutron star.

All of the objects in Table 4 except the central star in RCW 103 and the candidate progenitor of PKS 1209–52 have shown pulsations in at least one energy band. PSR 0656 + 14 most resembles PSR 1055–52 in its properties; their rotational energy loss rates, X-ray luminosities, and X-ray spectra are similar. PSR 1055–52 may be extended by $\sim 10''$ (Cheng and

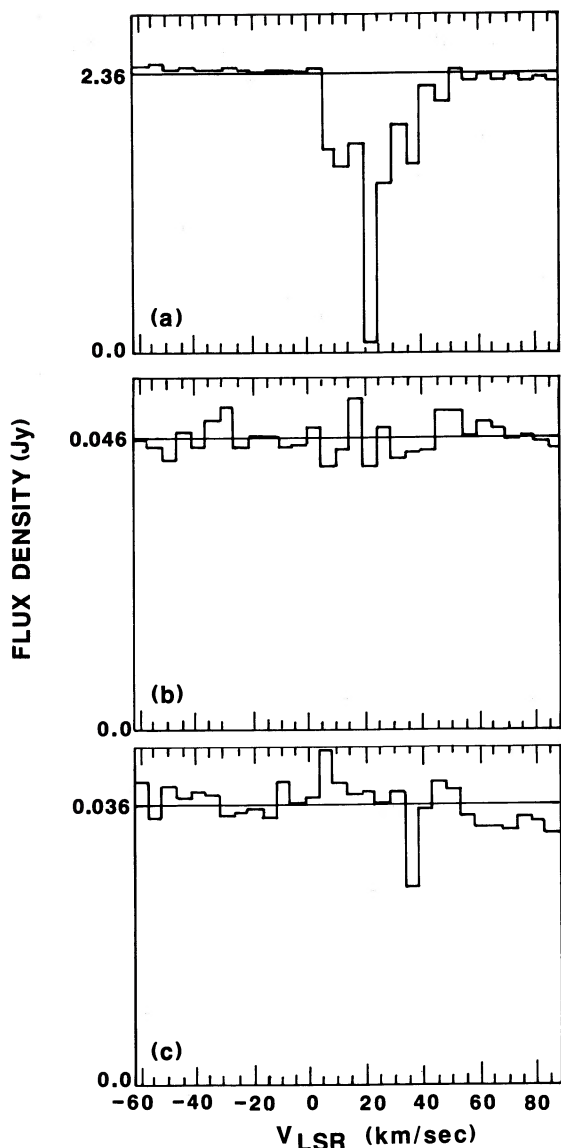


FIG. 10.—H I absorption spectra, normalized by dividing the flux density for each frequency channel by the continuum flux for each source, for (a) the calibrator 0622+147; (b) the elongated 2:1 radio source south of PSR 0656+14; and (c) the second brightest source complex in the field, which is 6' south and 6' west of the pulsar.

Helfand 1983, but see also Seward and Wang 1988), but, as we have shown, there is no evidence for a similar extent in PSR 0656+14.

Further X-ray timing observations are needed to confirm whether PSR 0656+14 can join the company of the three known isolated X-ray pulsars: the Crab, the LMC pulsar, and PSR 1509–58. The radio period of PSR 0656+14 is somewhat smaller than the norm among radio pulsars; the combination of this period and its relatively high period derivative give a characteristic spin-down age of 1.1×10^5 yr. This makes PSR 0656+14 of “intermediate” age; it is relatively young among the bulk of known radio pulsars, but still about 100 times older than the dozen or so youngest known pulsars. The period and period derivative of PSR 0656+14 can also be used to derive the rotational energy loss rate of the pulsar ($\dot{E} \propto \dot{P}/P^3$). This rate, 4×10^{34} ergs s^{-1} , is easily high enough to

power the X-ray luminosity of the pulsar. The surface magnetic field implied by the pulse parameters [i.e., $B \propto (P\dot{P})^{1/2}$] is 4.6×10^{12} G.

Table 4 also summarizes the X-ray data on these 12 objects. Two spectral indicators are listed for each source, where this information is available. (As indicated in the table, for some objects the IPC spectral data for the point source is contaminated by a surrounding, X-ray-emitting synchrotron nebula). The spectral indicators are the ratio of HRI to IPC counts, and the IPC “hardness ratio,” defined as the hard band counts (0.8–3.5 keV) minus the soft band counts (0.2–0.8 keV), divided by the sum of the soft and hard band counts. We note that in the published literature these parameters are often defined differently and often use *Einstein* IPC data which were processed at different times, and hence with different algorithms. For more accurate comparison, the X-ray data used for Table 4 were recomputed by us using IPC and HRI data with the most current data processing algorithms. The ratio of HRI to IPC counts for PSR 0656+14 is the highest among the isolated neutron stars detected with *Einstein*, and the IPC “hardness ratio” is the most negative. In fact, most of the isolated neutron stars in Table 4 have much harder X-ray spectra than PSR 0656+14 (see references in Table 4). Geminga and PSR 1055+52 may have spectra that are as soft as PSR 0656+14, but are more absorbed.

PSR 0656+14 does not appear as a gamma-ray source in either the First or Second Catalog of *COS B* sources (see Swanenburg *et al.* 1981). The fact that there is no optical counterpart to the pulsar is not surprising if the X-ray emission is, indeed, thermal radiation from the neutron star. A 30 eV unabsorbed blackbody would be a 28th mag object in the *V* band. On the other hand, a continuation of a power-law spectrum with $\alpha = 4$ to the optical would imply a 2d mag object, clearly not observed. Thus, if the true X-ray spectrum is a power law it must turn over in the UV or EUV.

b) PSR 0656+14: The Possible Progenitor of the Monogem Remnant?

One of the most exciting aspects of PSR 0656+14 is the possibility that it is associated with an extended, soft X-ray emission feature in Gemini-Monoceros (a.k.a. Monogem remnant). This $\sim 20^\circ$ diameter “ring” was first detected in a rocket flight that mapped the diffuse soft X-ray background (Bunner *et al.* 1971). The low-energy detectors on the A-2 experiment on *HEAO 1* were able to take a much longer look at the feature and, in examining possible origins for the ring, Nousek *et al.* (1981) favored the notion that it was a field supernova remnant. Fink (1989) finds that both the ring and its center have the same spectral shape, which can be fitted with a Raymond and Smith plasma model having $T = 2.1 \times 10^6$ K. Fink finds that the upper limit to the column density of the ring and its center is 6×10^{19} cm^{-2} . The ring is very symmetric in shape, with fainter X-ray emission in the Galactic plane.

Nousek *et al.* (1981) noted that the radio pulsar PSR 0656+14 lies inside the ring, but at that time there was no other support for an association of the X-ray ring with the radio pulsar. Two pieces of information which came later from radio observations alone now make this association tenable: (1) the dispersion measure of the pulsar suggests that the distance of the pulsar is comparable to that estimated for the X-ray ring by Nousek *et al.*, i.e., 300 pc and (2) the more accurate period derivative for the radio pulsar (Domingue *et al.* 1986) gives a

TABLE 4
 X-RAY-EMITTING ISOLATED NEUTRON STARS

Object	SNR Associations ^(a)	p ^(b) (s)	\dot{p} (10^{-15} s s ⁻¹)	\dot{E} ($\times 10^{36}$ erg s ⁻¹)	τ (10^3 yr)	DM (cm ⁻³ pc)	d (kpc)
PSR 0531+21	Crab (p)	0.033 γ, x, o, r	422	500	1.23	57	2.0
PSR 0540-69	LMC (p)	0.050 x, o	479	150	1.66	...	55
0630+17	Geminga (†)	60 γ, x	4×10^6	0.0007
PSR 0656+14	Monogem (?)	0.385 $x?, r$	54	0.04	110	14	0.40
PSR 0833-45	Vela (c)	0.089 γ, o, r	124	7	11	69	0.50
PSR 0950+08	...	0.253 r	0.23	0.0006	17400	3.0	0.13
PSR 1055-52	... (p?)	0.197 r	5.83	0.03	537	30.1	0.95
1209-52	PKS 1209 (s)	20	...	2
PSR 1509-58	MSH 15-52 (c)	0.150 x, r	1540	18	1.55	235	4.2
1613-50	RCW 103 (s)	1	...	3.3
PSR 1929+10	...	0.227 r	1.16	0.004	3100	3.2	0.05
PSR 1951+32	CTB 80 (c)	0.0395 r	5.92	3.8	105	45	3.0

Object	IPC ct rate ^(c) (0.2-3.5 keV)	HR ^(d)	HRI/IPC ^(e)	$L_x^{(f)}/L_{opt}$	L_γ/L_x	Refs.
PSR 0531+21	100	0.3	1
PSR 0540-69	(0.12)	0.58 ^(g)	...	250	...	2, 3
0630+17	0.115	-0.67	0.58	1800	1000	4, 5
PSR 0656+14	0.365	-0.78	0.74	>1800	...	6
PSR 0833-45	1.197	0.12	...	3200	1000	7
PSR 0950+08	0.0065	-0.05	6, 8
PSR 1055-52	0.088	-0.66	0.57	9, 10
1209-52	0.060	0.33	11
PSR 1509-58	0.273	0.69	0.04	12, 13
1613-50	14
PSR 1929+10	0.003	1.0	0.27	8, 15
PSR 1951+32	(0.10)	0.59 ^(g)	(0.075)	16, 17

^a Type: (p) for plerion, (c) for composite, (s) for shell, (†) for other.

^b Pulsations detected in γ (gamma-ray), X (X-ray), o (optical), r (radio).

^c X-radiation from the Crab Nebula (684 counts s^{-1} ; Seward 1988, private communication) saturated the telemetry capability of the IPC (128 counts s^{-1}) so that it is not possible to obtain an IPC count rate for the pulsar. Values in parentheses indicate rough estimates. The rate given for the LMC pulsar is for the pulsed component of the SNR. RCW 103 was not detected in the IPC because of the high diffuse background of the SNR. The point source contribution of PSR 1951 + 32 to the CTB 80 remnant is inferred from the radial distribution of surface brightness (Wang and Seward 1984).

^d HR is "hardness ratio" = (hard - soft count rates)/(hard + soft count rates), where hard = 0.8-4 keV and soft = 0.2-0.8 keV.

^e HRI/IPC = ratio of counts in these two detectors. Several objects were not detected in the HRI. RCW 103 was detected *only* in HRI at a rate of 3.8 s^{-1} . The Crab pulsar was detected at 4.7 s^{-1} in the HRI. The value for PSR 1951 + 32 was computed by Seward and Wang 1988.

^f L_x is the time-averaged luminosity of the compact star.

^g Contaminated by enveloping SNR. Used spectral parameters from referenced papers to calculate.

REFERENCES.—References are chiefly for X-ray detections. Most of the radio references, except as noted, are in Manchester and Taylor 1981. (1) Harnden and Seward 1984; (2) Seward, Harnden, and Helfand 1984; (3) Middleditch and Pennypacker 1985 (optical); (4) Bignami 1987 (review); (5) Halpern and Tytler 1988; (6) this paper; (7) Harnden *et al.* 1985; (8) Helfand 1983; (9) Cheng and Helfand 1983; (10) Brinkmann and Ögelman 1987; (11) Kellett *et al.* 1987; (12) Seward and Harnden 1982; (13) Manchester, Tuohy, and D'Amico 1982 (radio); (14) Tuohy and Garmire 1980; (15) Alpar *et al.* 1987; (16) Wang and Seward 1984; (17) Clifton *et al.* 1987 (radio).

characteristic spin-down age (1.1×10^5 yr) for the pulsar that is consistent with the approximate age of 6×10^4 yr derived for the X-ray ring by Nousek *et al.* The pulsar is located approximately 5° from the center of the ring. (See Nousek *et al.* for a schematic diagram of the ring and the pulsar's location with respect to its center.) For a distance of 300 pc, this displacement corresponds to a transverse pulsar velocity of about 230 km s^{-1} , a high, but not extraordinary value for pulsars.

The interstellar scintillation velocity, v_{ISS} , of the pulsar, however, has been recently measured as 36 ± 10 km s^{-1} (A. Wolszczan 1988, private communication). This is a measurement of the transverse component of the pulsar's velocity and has an undetermined direction. If it represents the pulsar's true space velocity, both the pulsar and the Monogem remnant would have to be at a distance ~ 50 pc to be associated with each other (i.e., for a pulsar origin at the geometric center of this apparently symmetric ring). A distance as small as 50 pc is problematic because it would imply that if the Monogem remnant resulted from an explosion of the pulsar's progenitor 10^5 years ago, it had an expansion velocity of only ~ 100 km

s^{-1} , far lower than a typical SNR. The interstellar scintillation velocity may be an underestimate of the pulsar's space velocity if the scattering material along the line of sight is not uniform. A good correlation of space velocity with $P\dot{P}$ has been found for a large number of pulsars (Cordes 1986). In the case of PSR 0656 + 14, v_{ISS} is so low that if it is used as the pulsar's true space velocity, this pulsar does not fit the correlation well. This result motivates astrometry of PSR 0656 + 14 to determine its proper-motion speed. In addition, further observations in the IR and radio are needed to confirm that the X-ray ring is, in fact, a SNR.

c) Associations of PSR 0656 + 14 with the Other Nearby Radio Sources

Radio-bright synchrotron nebulae have been found surrounding several radio pulsars. The Crab Nebula is the most prominent example. While neither our X-ray, optical, nor radio images to date have revealed extended emission surrounding PSR 0656 + 14, Figure 9 shows that there is much extended radio emission relatively nearby (1.2 - 3.3 away). No

X-ray emission is detected at this location with a 3σ upper limit, as determined from the HRI image, of 2% of the flux of the pulsar itself.

The most important thing about the extended radio source is that part of it is 40%–50% linearly polarized; this establishes the emission to be synchrotron radiation. Most background sources are unpolarized or only have polarizations up to several percent, but linear polarization of $\sim 50\%$ in the lobes of double radio sources is occasionally encountered (Kellermann and Owen 1988). There is no obvious elliptical galaxy on the optical image (Fig. 1) at the position of the extended radio source. There are, however, two apparently pointlike sources that coincide with interesting positions in the radio contour map. A comparison of Figure 1 with Figure 8*b* shows that one object is located in the “hole” between the two extended sources of Figure 8*b* (which, as Fig. 9 illustrates, actually make up one elongated source), while the second optical object is located in one of the bright knots of the extended radio source at the center of Figure 8*b*. These optical objects are indicated by numbers “1” and “2,” respectively, on the image of the CCD *V* frame (Fig. 1) and, for comparison, on the Stokes *I* parameter plot (Fig. 8*b*). The *V* and *R* magnitudes of object 1 are 18.6 and ≤ 18.3 , respectively, and 22.4 and 20.6 for object 2. The *I* magnitude of object 2 is 19.1. Optical spectroscopy of both of these objects is needed to determine any association with the extended radio source.

The low measurement of H I absorption against the extended radio source, as well as its high linear polarization, suggests that this emission could be a Galactic synchrotron nebulosity, and may be associated with the pulsar. If both the pulsar and the extended source are at a distance of 300 pc, they lie only 0.27 pc from each other and one can infer a relative transverse velocity of only 2.6 km s^{-1} . The extended source could be plerionic in nature, much like the nebular radio emission associated with the Vela pulsar. The few radio and X-ray-emitting nebulae discovered in association with pulsars are thought to be evidence for a relativistic wind from the pulsar that carries a toroidal magnetic field into a surrounding nebula, which then emits synchrotron radiation. If the extended radio source nearby PSR 0656+14 were plerionic, it would be unusual among the known plerions which have pulsars with much higher energy loss rates (see § *Vd* below).

An alternative possibility is that the extended radio feature is a region of enhanced density with embedded magnetic fields near the pulsar, which is energized by a wind of relativistic charged particles from the pulsar. A “radio halo” of dimensions ≤ 1 pc has been predicted by Blandford *et al.* (1973). Deep radio continuum images with comparable spatial information at two or more frequencies are desirable to see if the extended source has the expected flat spectral characteristics. The relationship between the pulsar, the diffuse radio region, and the Monogem remnant could also be examined with radio astrometry. We note that the extended region, which is linear in shape, is not aligned along a radius from the center of the Monogem remnant to the pulsar, but is positioned nearly perpendicular to such a radius (in the Galactic coordinate frame depicted in Nousek *et al.* 1981). Thus, if the pulsar, the Monogem remnant, and the extended feature near the pulsar are all related, the pulsar will be travelling radially away from the center of the Monogem remnant, at an oblique angle to the linearly extended feature. This may imply that the gas responsible for the latter is not expelled from the pulsar, but is a clump of dense material serendipitously located near enough to the pulsar to be energized by its particle emission.

d) X-Radiation from the Heated Neutron Star Surface?

Here we consider the origin of the observed X-ray emission, examining first the possibility that it is synchrotron radiation. Extended X-ray synchrotron nebulae are associated with some of the isolated neutron stars in Table 4, but only when $\dot{E} \geq 0.1 \times 10^{36} \text{ ergs s}^{-1}$. This would seem to indicate (see Seward and Wang 1988) that for lower values of \dot{E} a pulsar cannot power an intense nebula (complicating the question of the nature of the nearby extended radio source!). The X-ray spectral data on PSR 0656+14 allow a steep power-law spectrum, which would be a sign of synchrotron nebular emission, but the spatial data require that its size be $\leq 5''$. This is small compared to that of known X-ray synchrotron nebulae. As mentioned previously, if a power-law spectrum applies to the data there must be a turnover in the injected electron spectrum in the UV or EUV or an optical synchrotron nebula would have been detected. A further difficulty with the X-ray synchrotron interpretation, analogous to that made by Brinkmann and Ögelman (1987; see also references therein) for PSR 1055–52, which has X-ray spectral properties similar to those of PSR 0656+14, is that the observed energy spectral index of $\alpha \geq 2.6$ implies a steep spectrum that has heretofore not been observed in Crab-like remnants and is not expected from theoretical estimates of the spectra of synchrotron nebulae created by pulsars.

We therefore find attractive an alternative possibility: that all of the detected X-ray emission is thermal radiation from the surface of the neutron star. The X-ray spectral data suggest for this case, assuming the distance to PSR 0656+14 to be 400 pc, that $kT \sim 50 \text{ eV}$, that N_{H} is low ($\leq 10^{18} \text{ cm}^{-2}$), and that the bolometric luminosity is of order $10^{32} \text{ ergs s}^{-1}$. Lower temperatures and higher columns (up to $N_{\text{H}} = 10^{20} \text{ cm}^{-2}$) are allowed if the source is closer than 400 pc. The range of permissible temperatures is the same as that measured for PSR 1055–52 (Brinkmann and Ögelman 1987). The equivalent hydrogen column density to PSR 1055–52 ($\sim 10^{20} \text{ cm}^{-2}$), however, may be an order of magnitude higher than for PSR 0656+14. (If the latter had a similar column of 10^{20} cm^{-2} , its temperature must be more like 30 eV and the distance more like 100 pc; see Figs. 2 and 3). Ways of “reheating” an aging neutron star (e.g., energy dissipation by torques internal to the neutron star, or polar cap heating due to energetic particles from the magnetosphere infalling onto the neutron star) are considered by Brinkmann and Ögelman (1987; see also references therein) for PSR 1055–52 and found wanting because they cannot produce the observed temperature or luminosity. Similar arguments apply to PSR 0656+14, whose dynamical age, like that of PSR 1055–52, is young enough (i.e., 10^5 yr) that its observed temperature may be an indication that it is still cooling from its initial explosion.

e) PSR 0656+14 and Limits to the Flux Density of Magnetic Monopoles

X-ray observations of individual compact stars as well as the diffuse sky background can be used to set interesting limits on F_M , the flux density of magnetic monopoles (Kolb and Turner 1984). The original motivation for the ultrasoft X-ray survey of the *Einstein* sky described in the Introduction to this paper (see also Córdova, Bell, and Kolb 1985) was to set such a limit by searching for isolated neutron stars kept hot ($kT \sim 30 \text{ eV}$) by monopole catalysis of nucleon decay (e.g., Kolb, Colgate, and Harvey 1982). The nondetection of such objects could be used to bound the photon luminosity of such sources and hence limit the flux density of magnetic monopoles predicted in

certain grand unified theories. This limit would be at least seven orders of magnitude lower than the limit derived from the survival of Galactic magnetic fields. Our long-term plan is to improve on an earlier survey that involved only a small area on the sky (Kolb, Colgate, and Harvey 1982) by using the entire *Einstein* data base, which covers about 8% of the sky. In principle, however, X-ray detections of isolated neutron stars such as PSR 0656+14 could also give a bound on monopole catalysis of nucleon decay. For example, Freese, Turner, and Schramm (1983) used an *Einstein* X-ray detection of the radio pulsar PSR 1929+10 (Helfand 1983) to provide a limit, $F_M(\sigma_0 \beta) \leq 7 \times 10^{-22} \text{ cm}^{-2} \text{ sr}^{-2} \text{ s}^{-1}$ (where $10^{-28} \times \sigma_0 \beta \text{ cm}^2$ is the product of the catalysis cross section and the nucleon-monopole relative velocity). This limit becomes more than six orders of magnitude better when consideration is taken of the pulsar's lifetime as a progenitor star on the main sequence. Since the X-ray luminosity of PSR 1929+10 is $\sim 10^4$ times less than that of PSR 0656+14, and it is 30 times older (i.e., has had more time to accrete monopoles), the limit of Freese *et al.* is not improved with the detection of PSR 0656+14. This is true even if the X-ray emission detected from PSR 1929+10 using the *Einstein* satellite is hard, rather than soft as assumed by Freese *et al.* In fact, the ratio of the HRI to IPC flux for PSR 1929+10 (Table 4) and a nondetection with the *EXOSAT* satellite (Alpar *et al.* 1987) suggests a spectrum for PSR 1929+10 that is much harder than that of PSR 0656+14. Alpar *et al.* (1987) put a limit on the blackbody temperature of PSR 1929+10 of $2 \times 10^5 \text{ K}$ for a neutron star with a radius of 10 km. This corresponds to a bolometric luminosity of $10^{30} \text{ ergs s}^{-1}$, which is still two orders of magnitude less than the blackbody luminosity of PSR 0656+14. Kolb and Turner (1984) compare the serendipitous source survey method, the individual source detection method of Freese, Turner, and Schramm, and other methods for deriving limits on the monopole flux. They conclude that each method involves uncertainties and weaknesses, but the uncertainties are different while the limits tend to be comparable, giving one confidence in the validity of the bound on the monopole flux density.

VI. FUTURE OBSERVATIONS

PSR 0656+14 could be singularly interesting among radio pulsars because it may be the compact remnant of the progenitor of the oldest SNR that has yet been detected in association with a known pulsar. It may thus be important in studying the evolution of SNRs, as well as the cooling history of pulsars. The extremely soft X-ray spectrum of both the pulsar and its remnant may be important aspects of this evolution.

There are several important future observations that should be made of the pulsar and its environs.

1. The suggestion in the data that PSR 0656+14 might be an X-ray pulsar is one that can be easily verified with the X-ray focal plane instruments on the upcoming ROSAT satellite. It would be only the fourth X-ray pulsar among the radio pulsars and valuable for understanding the beaming geometry of pulsars. More detailed X-ray spectroscopy with ROSAT is essential for understanding the nature of pulsar X-radiation.

2. The apparent column to the source is low enough that pulsations should also be searched for in the extreme ultraviolet with ROSAT's XUV Wide Field Camera and NASA's Extreme Ultraviolet Explorer telescope. If detected, this would mark an unprecedented opportunity to study the pulsation spectrum of a pulsar over a wide frequency range.

3. The region surrounding PSR 0656+14 needs further

study to determine if there is more extended or filamentary radio emission associated with the pulsar. Simultaneous observations of the average continuum emission and pulsed emission from the pulsar are needed to determine if there is plerionic emission surrounding the pulsar. The pulsar and the nearby extended radio source illustrated in Figure 9 should be examined using radio continuum mapping with similar resolutions at 6 cm and 20 cm for evidence of structure connecting these sources. The extended emission needs more sensitive, low-resolution images in total intensity, linear polarization, and spectral index. It would be valuable, for example, to determine if it has the flat spectrum characteristic of a plerionic source. The possibility of unusually low N_{H}/T_s for the line-of-sight column density in the Monogem remnant, due to unusually high T_s , should be explored by H I absorption experiments against some of the many strong background sources in the vicinity of the Monogem remnant. Optical spectroscopy should be done on sources located in interesting regions of the radio map of the extended source.

4. The Monogem remnant should be studied in the infrared, using *IRAS* data, to attempt to verify the supernova remnant nature of the feature. A SNR could show infrared emission that is spatially correlated with the X-ray emission. A detection would allow us to study the effects of dust cooling on an aging SNR. The more recent radio surveys should be also examined for correlations with the X-ray ring.

5. A deep search should be made at optical wavelengths for the counterpart of the pulsar and a possible nebular component. The detection of an optical source would constrain models for the X-ray emission. Optical pulsations would give new information on pulsar beaming models.

6. A determination of the transverse motion of the pulsar could be made with radio interferometry. This would give us information about the dynamics of the original explosion. Radio astrometry would give us a better knowledge of how fast pulsars are escaping from the Galactic plane and the kinematic age of pulsars in general. The latter is a better estimate of the true age and, in comparison with the spin-down age (which is actually an upper limit to a pulsar's age), is important for models of changes in the braking index and magnetic field of pulsars over their histories. Astrometry could help resolve the question of association of the pulsar with the Monogem remnant by determining the motion of the pulsar with respect to the center of the large, circular, X-ray-emitting ring. Finally, astrometry could also be used to further explore the relationship of the pulsar to the extended radio emission that lies within a few arcminutes of the pulsar.

F. A. C. is indebted to Rocky Kolb for starting her on a search for isolated, hot neutron stars, and to Ted Rodriguez-Bell for work on the preliminary soft *Einstein* survey, which produced the "interesting" candidate that is the subject of this paper. Fred Seward, Susan Gibbs Hazelton, and Chris Mauche are thanked for helping with various software aspects of the X-ray data analysis, and Fred also for sharing his wisdom on X-ray-emitting pulsars in general. Alex Wolszczan kindly supplied the pulsar scintillation measurement, Jeremy Mould an upper limit to the pulsar's R magnitude, Tony Stark the data on the average 21 cm line-of-sight column density in the pulsar's direction, and Richard Fink and John Nousek updated analysis of the *HEAO 1* X-ray data on the Gemini-Monoceros enhancement. We thank Roger Romani and Jonathan Arons for insight and discussions, and Richard Epstein

and Chris Mauche for critiquing the original manuscript. We also thank the staff of the La Palma observatory who obtained the CCD images of the PSR 0656+14 field as part of the service observing program. F. A. C. is grateful for support from

NASA's Astrophysics Data Program. K. O. M. acknowledges the support of the Royal Society of London. The US Department of Energy also provided support to F. A. C. and J. M.

REFERENCES

- Alpar, A., Brinkmann, W., Kiziloğlu, U., Ögelman, H., and Pines, D. 1987, *Astr. Ap.*, **177**, 101.
- Becker, R. H., Helfand, D. J., and Szymkowiak, A. E. 1982, *Ap. J.*, **255**, 557.
- Bignami, G. F. 1987, in *The Origin and Evolution of Neutron Stars*, ed. D. J. Helfand and J. H. Huang (Dordrecht: Reidel), p. 465.
- Blandford, R. D., Ostriker, J. P., Pacini, F., and Rees, M. J. 1973, *Astr. Ap.*, **23**, 145.
- Brinkmann, W., and Ögelman, H. 1987, *Astr. Ap.*, **182**, 71.
- Bunner, A. N., Coleman, P. L., Kraushaar, W. L., and McCammon, D. 1971, *Ap. J.*, **167**, L3.
- Cheng, A. F., and Helfand, D. J. 1983, *Ap. J.*, **271**, 271.
- Clifton, T. R., Backer, D. C., Foster, R. S., Kulkarni, S. R., Fruchter, A. S., and Taylor, J. H. 1987, *IAU Circ.*, No. 4422.
- Cordes, J. M. 1986, *Ap. J.*, **311**, 183.
- Córdova, F. A., Bell, T., and Kolb, E. 1985, *Bull. AAS*, **17**, 906.
- Córdova, F. A., Hjellming, R. M., Mason, K. O. and Middleditch, J. 1987, *IAU Circ.*, No. 4490.
- Córdova, F. A., Kartje, J., Mason, K. O., and Harnden, F. R. 1989, in *Berkeley Colloquium on Extreme Ultraviolet Astronomy*, ed. R. F. Malina and S. Bowyer (Elmsford, N.Y.: Pergamon Press), in press.
- Dewey, R. J., Taylor, J. H., Maquire, C. M., and Stokes, G. H. 1988, *Ap. J.*, **332**, 762.
- Domingue, D., Rankin, J. M., Weisberg, J. M., and Backus, P. R. 1986, *Astr. Ap.*, **161**, 303.
- Fink, R. 1989, Ph.D. thesis, Pennsylvania State University.
- Freese, K., Turner, M. S., and Schramm, D. N. 1983, *Phys. Rev. Letters*, **51**, 1625.
- Giacconi, R., et al. 1979, *Ap. J.*, **230**, 540.
- Gundmundsson, E. H., Pethick, C. J., and Epstein, R. I. 1983, *Ap. J.*, **272**, 286.
- Halpern, J. P., and Tytler, D. 1988, *Ap. J.*, **330**, 201.
- Harnden, F. R., Jr., Grant, P. D., Seward, F. D., and Kahn, S. M. 1985, *Ap. J.*, **299**, 828.
- Harnden, F. R., Jr., and Seward, F. D. 1984, *Ap. J.*, **283**, 274.
- Helfand, D. J. 1983, in *IAU Symposium 101, Supernova Remnants and Their X-Ray Emission*, ed. J. Danziger and P. Gorenstein (Dordrecht: Reidel), p. 471.
- Hertz, P. 1983, Ph.D. thesis, Harvard University.
- Kellerman, K. I., and Owen, F. N. 1988, in *Galactic and Extra-Galactic Radio Astronomy*, ed. G. L. Verschuur and K. I. Kellermann (2d ed.; Berlin: Springer), p. 563.
- Kellett, B. J., Branduardi-Raymont, G., Culhane, J. L., Mason, I. M., Mason, K. O., and Whitehouse, D. R. 1987, *M.N.R.A.S.*, **225**, 199.
- Kholopov, P. N., et al. 1985, in *General Catalogue of Variable Stars* (4th ed.; Moscow: Nauka) (GCVS).
- Kolb, E. W., Colgate, S. A., and Harvey, J. A. 1982, *Phys. Rev. Letters*, **49**, 1373.
- Kolb, E. W., and Turner, M. S. 1984, *Ap. J.*, **286**, 71.
- Kulkarni, S., and Heiles, C. E. 1988, in *Galactic and Extra-Galactic Radio Astronomy*, ed. G. L. Verschuur and K. I. Kellermann, (2d ed.; Berlin: Springer), p. 95.
- Lampton, M., Margon, B., and Bowyer, S. 1976, *Ap. J.*, **208**, 177.
- Maccacaro, T., et al. 1982, *Ap. J.*, **253**, 504.
- Manchester, R. N., Lyne, A. G., Taylor, J. H., Durdin, J. M., Large, M. I., and Little, A. G. 1978, *M.N.R.A.S.*, **185**, 409.
- Manchester, R. N., and Taylor, J. H. 1981, *A.J.*, **86**, 1953.
- Manchester, R. N., Tuohy, I. R., and D'Amico, N. 1982, *Ap. J. (Letters)*, **262**, L31.
- Middleditch, J., and Pennypacker, C. R. 1985, *Nature*, **313**, 659.
- Nelson, R. F., and Spencer, R. E. 1988, *M.N.R.A.S.*, **234**, 1105.
- Nousek, J. A., Cowie, L. L., Hu, E., Lindblad, C. J., and Garmire, G. P. 1981, *Ap. J.*, **248**, 152.
- Pandharipande, V. R., and Smith, R. A. 1975, *Nucl. Phys.*, **A237**, 507.
- Seward, F. D., and Harnden, F. R., Jr. 1982, *Ap. J. (Letters)*, **256**, L45.
- Seward, F. D., Harnden, F. R., Jr., and Helfand, D. J. 1984, *Ap. J. (Letters)*, **287**, L19.
- Seward, F. D., and Wang, Z-R. 1988, *Ap. J.*, **332**, 199.
- Swanenburg, B. N., et al. 1981, *Ap. J. (Letters)*, **243**, L69.
- Tuohy, I., and Garmire, G. 1980, *Ap. J. (Letters)*, **239**, L107.
- Wang, Z. R., and Seward, F. D. 1984, *Ap. J.*, **285**, 607.
- Weaver, H. F., and Williams, D. R. W. 1973, *Astr. Ap.*, **8**, 1.

F. A. CORDOVA: MS D436, Los Alamos National Laboratory, Los Alamos, NM 87545

R. M. HJELLMING: National Radio Astronomy Observatory, P.O. Box 0, Socorro, NM 87801

K. O. MASON: Mullard Space Science Laboratory, Holmbury St. Mary, Dorking, Surrey, RH5 6NT, U.K.

J. MIDDLEDITCH: MS B265, Los Alamos National Laboratory, Los Alamos, NM 87545